



## Understanding the Effect of Hydration on the Bio-inert Properties of 2-Hydroxyethyl Methacrylate Copolymers with Small Amounts of Amino- or/and Fluorine-Containing Monomers

Koguchi, Ryohei; Jankova, Katja; Hayasaka, Yuki; Kobayashi, Daisuke; Amino, Yosuke; Miyajima, Tatsuya; Kobayashi, Shingo; Murakami, Daiki; Yamamoto, Kyoko; Tanaka, Masaru

*Published in:*  
A C S Biomaterials Science & Engineering

*Link to article, DOI:*  
[10.1021/acsbmaterials.0c00230](https://doi.org/10.1021/acsbmaterials.0c00230)

*Publication date:*  
2020

*Document Version*  
Peer reviewed version

[Link back to DTU Orbit](#)

*Citation (APA):*  
Koguchi, R., Jankova, K., Hayasaka, Y., Kobayashi, D., Amino, Y., Miyajima, T., Kobayashi, S., Murakami, D., Yamamoto, K., & Tanaka, M. (2020). Understanding the Effect of Hydration on the Bio-inert Properties of 2-Hydroxyethyl Methacrylate Copolymers with Small Amounts of Amino- or/and Fluorine-Containing Monomers. *A C S Biomaterials Science & Engineering*, 6(5), 2855-2866. <https://doi.org/10.1021/acsbmaterials.0c00230>

---

### General rights

Copyright and moral rights for the publications made accessible in the public portal are retained by the authors and/or other copyright owners and it is a condition of accessing publications that users recognise and abide by the legal requirements associated with these rights.

- Users may download and print one copy of any publication from the public portal for the purpose of private study or research.
- You may not further distribute the material or use it for any profit-making activity or commercial gain
- You may freely distribute the URL identifying the publication in the public portal

If you believe that this document breaches copyright please contact us providing details, and we will remove access to the work immediately and investigate your claim.

This document is confidential and is proprietary to the American Chemical Society and its authors. Do not copy or disclose without written permission. If you have received this item in error, notify the sender and delete all copies.

**Understanding the effect of hydration on the bio-inert properties of HEMA copolymers with small amounts of amino- or/and fluorine-containing monomers**

Journal:	<i>ACS Biomaterials Science &amp; Engineering</i>
Manuscript ID	ab-2020-002302.R2
Manuscript Type:	Article
Date Submitted by the Author:	18-Mar-2020
Complete List of Authors:	Koguchi, Ryohei; AGC Inc. , New Product R&D Center Jankova, Katja; Technical University of Denmark, Energy Conversion and Storage Hayasaka, Yuki; AGC Inc. , Innovative Technology Research Center Kobayashi, Daisuke; AGC Inc. , Innovative Technology Research Center Amino, Yosuke ; AGC Inc. , Innovative Technology Research Center Miyajima, Tatsuya; AGC, Ltd., Kobayashi, Shingo; Kyushu University, Chemistry Murakami, Daiki; Kyushu University , Yamamoto, Kyoko; AGC Inc. , New Product R&D Center Tanaka, Masaru; Kyushu University, Chemistry

SCHOLARONE™  
Manuscripts

1  
2  
3  
4  
5  
6  
7  
8  
9  
10  
11  
12  
13  
14  
15  
16  
17  
18  
19  
20  
21  
22

# Understanding the effect of hydration on the bio-inert properties of HEMA copolymers with small amounts of amino- or/and fluorine-containing monomers

23  
24  
25  
26  
27  
28  
29  
30  
31  
32  
33  
34  
35  
36  
37  
38  
39  
40  
41  
42  
43  
44  
45

*Ryohei Koguchi,<sup>1,3</sup> Katja Jankova,<sup>2,4</sup> Yuki Hayasaka,<sup>5</sup> Daisuke Kobayashi,<sup>5</sup> Yosuke Amino,<sup>5</sup> Tatsuya Miyajima,<sup>5</sup> Shingo Kobayashi,<sup>2</sup> Daiki Murakami,<sup>1,2</sup> Kyoko Yamamoto,<sup>3</sup> Masaru Tanaka<sup>1,2\*\*</sup>*

46  
47  
48  
49  
50  
51  
52  
53  
54  
55  
56  
57  
58  
59  
60

**Dedicated to the 100 years' birthday (01.01.2020) of prof. Teiji Tsuruta**

<sup>1</sup> Graduate School of Engineering, Kyushu University, 744 Motooka, Nishi-ku, Fukuoka 819-0395, Japan.

<sup>2</sup> Soft Materials Chemistry, Institute for Materials Chemistry and Engineering, Kyushu University, Build. CE41, 744 Motooka Nishi-ku, Fukuoka, 819-0395, Japan

<sup>3</sup> AGC Inc. Organic Materials Division, Materials Integration Laboratories, 1150 Hazawa-cho, Kanagawa-ku, Yokohama, Kanagawa 221-8755, Japan

<sup>4</sup> Department of Energy Conversion and Storage, Technical University of Denmark, Fysikvej, Build. 375, 2800 Kongens Lyngby, Denmark

<sup>5</sup> AGC Inc. Common Base Technology Division, Innovative Technology Laboratories, 1150 Hazawa-cho, Kanagawa-ku, Yokohama, Kanagawa 221-8755, Japan

**Corresponding Author**

1  
2  
3  
4 \*E-mail: masaru\_tanaka@ms.ifoc.kyushu-u.ac.jp  
5  
6  
7  
8  
9  
10  
11  
12  
13  
14  
15  
16  
17  
18  
19  
20  
21  
22  
23  
24  
25  
26  
27  
28  
29  
30  
31  
32  
33  
34  
35  
36  
37  
38  
39  
40  
41  
42  
43  
44  
45  
46  
47  
48  
49  
50  
51  
52  
53  
54  
55  
56  
57  
58  
59  
60

1  
2  
3 **Abstract:** Materials exhibiting "bio-inert properties" are essential for developing medical  
4  
5  
6 devices, because they are less recognized as foreign substances by proteins and cells in  
7  
8 the living body. We have reported that the presence of intermediate water (*IW*), the water  
9  
10 molecules loosely bound to a polymer, is a useful index of the bio-inertness of materials.  
11  
12 Here, we analyzed the hydration state and the responses to biomolecules of poly(2-  
13  
14 hydroxyethyl methacrylate) (PHEMA) copolymers including small amounts of 2-  
15  
16 (dimethylamino)ethyl methacrylate (DMAEMA) (N-series) or/and 2,2,2-trifluoroethyl  
17  
18 methacrylate (TFEMA) (F-series). The hydration structure was analyzed by differential  
19  
20 scanning calorimetry (DSC), the molecular mobility of the produced copolymers by  
21  
22 temperature derivative of DSC (DDSC), and the water mobility by solid  $^1\text{H}$  pulse nuclear  
23  
24 magnetic resonance (NMR). Although the homopolymers did not show bio-inert  
25  
26 properties, the binary and ternary PHEMA copolymers with low comonomer contents  
27  
28 showed higher bio-inert properties than PHEMA homopolymer. The hydration state of  
29  
30 PHEMA was changed by introducing small amount of comonomers. The mobility of both,  
31  
32 water molecules and hydrated polymers was changed in the N-series, nonfreezing water  
33  
34 (*NFW*), the water molecules tightly bound to a polymer, was shifted to high mobility *IW*  
35  
36 and free water (*FW*), the water molecules scarcely bound to a polymer. On the other  
37  
38 hand, in the F-series, *FW* turned to *IW* and *NFW*. Additionally, a synergetic effect was  
39  
40 postulated when both comonomers coexist in the copolymers of HEMA, which was  
41  
42 expressed by widening the temperature range of cold crystallization, contributing to  
43  
44 further improvement of the bio-inert properties.  
45  
46  
47  
48  
49  
50  
51  
52  
53  
54  
55  
56  
57  
58  
59  
60

1  
2  
3  
4  
5  
6  
7 **KEYWORDS** Intermediate water, bio-inert, poly(2-hydroxyethyl methacrylate), hydration  
8  
9 state, fluorinated polymers, amino and fluorine.  
10  
11  
12  
13  
14  
15  
16  
17  
18  
19  
20  
21  
22  
23  
24  
25  
26  
27  
28  
29  
30  
31  
32  
33  
34  
35  
36  
37  
38  
39  
40  
41  
42  
43  
44  
45  
46  
47  
48  
49  
50  
51  
52  
53  
54  
55  
56  
57  
58  
59  
60

## Introduction

When any materials are implanted in the body, nonspecific protein adsorption may occur as a reaction to the foreign body. A number of different cells, such as platelets, adhere to these material surfaces and as a result this may lead to the upregulation of cytokines and subsequent proinflammatory processes.<sup>1</sup> To develop the implantable medical devices (e.g., stents, artificial blood vessel, artificial lung oxygenator, etc.), many efforts have been made to elucidate the expression mechanisms of bio-inert properties of materials – namely the mechanisms of low protein adsorption and cell adhesion inhibition.

Poly(ethylene glycol) (PEG)<sup>2</sup> and zwitterionic polymers<sup>3</sup> are the typical bio-inert polymers with the above mentioned properties. There are so many proposed mechanisms describing the properties originate from; it deems that the materials with high hydrophilicity often exhibit the properties. However, these homopolymers are limited in application because of their poor water resistance. Therefore, the polymers are generally used by improving the water resistance by copolymerizing with hydrophobic monomers or covalently grafting to a substrate, while these methods sacrifice the properties to some extent.

Han et al.<sup>4</sup> reported that poly(ethylene oxide)-grafted polyurethane surface showed lower fibrinogen and albumin adsorption than that of conventional polyurethane. The protein adsorption resistance property of the PEG-coated surface increases with increasing the density and length of the chains on the surface.<sup>5,6</sup> Nagasaki et al.<sup>7</sup> reported that the PEG graft density was enlarged by adding a filler layer made of low molecular weight PEG (2kDa) in the preconstructed high molecular weight PEG (5kDa) layer, which contributed to low protein adsorption. Similarly, Ishihara et al. reported that 2-methacryloyloxyethyl phosphorylcholine (MPC) can be used as a coating material by insolubilization either copolymerizing with hydrophobic butyl methacrylate<sup>8</sup>

1  
2  
3 or covalently bonding the MPC polymer to the surface.<sup>9</sup> PMPC-coated surfaces exhibit excellent  
4  
5 nonthrombogenicity to human whole blood.<sup>10</sup>  
6  
7

8 On the other hand, numerous investigations have been made to deepen the discussion not only on  
9  
10 the chemical structure of polymers but also on the polymer behavior at the water/polymer interface  
11  
12 including the interaction of the polymer with water. Poly(2-methoxyethyl acrylate) (PMEA) is a  
13  
14 water insoluble homopolymer with excellent blood compatibility, presumably due to the presence  
15  
16 of intermediate water (*IW*) – the water molecules that loosely bound to the polymer chain in the  
17  
18 hydrated state.<sup>11,12</sup> The blood compatibility of PMEA coated artificial lung (oxygenator) was  
19  
20 demonstrated in *in vitro* test and the compatibility was equivalent to that of heparin-immobilized  
21  
22 oxygenator because of its low plasma protein adsorption and denaturation.<sup>13</sup> PMEA coated  
23  
24 medical devices have thus been approved by the Food and Drug Administration (FDA) have  
25  
26 achieved clinical applications such as artificial lungs and catheters. In addition, systematic studies  
27  
28 were conducted with a variety of PMEA derivatives on clarifying the relationship between the  
29  
30 polymer structure, the *IW* contents (IWC), and the interactions with biomolecules.<sup>14,15,16</sup>  
31  
32 Consequently, the amount of *IW* in a hydrated polymer is gaining acceptance as a useful index of  
33  
34 the bio-inertness of the materials<sup>17</sup> rather than non-freezing water and free water.  
35  
36  
37  
38  
39  
40

41 Poly(2-hydroxyethyl methacrylate) (PHEMA) is one of the typical bio-inert materials, and many  
42  
43 researches have been conducted to study its properties as biomaterial. Since PHEMA has a  
44  
45 hydroxyl group in each monomer unit, it exhibits high hydrophilicity thanks to a high equilibrium  
46  
47 water content (EWC) of about 40 wt%. It has been utilized as a grafting material to the surfaces or  
48  
49 a hydrophilic unit in copolymers to give high hydrophilicity to materials. As examples of the  
50  
51 surface grafting with HEMA, silastic surfaces by Ratner et al.<sup>18</sup> and polyurethane film by Martins  
52  
53 et al.<sup>19</sup> are given. For random copolymers, ethyl methacrylate copolymer by Ratner and Hoffman  
54  
55  
56  
57  
58  
59  
60



1  
2  
3 et al.<sup>20</sup>, and block copolymer with styrene by Okano et al.<sup>21</sup> and Senshu et al.<sup>22,23</sup> are given as  
4  
5 examples.

6  
7  
8 Kikuchi et al.<sup>24</sup> investigated the retention behavior of blood cells (erythrocytes, lymphocytes, and  
9  
10 platelets) using the surface of poly[*N*-methyl-*N*-(4-vinylphenethyl)ethylenediamine-*co*-2-  
11  
12 hydroxyethyl methacrylate] (HAV copolymer). The authors showed that the adhesion of  
13  
14 lymphocytes was suppressed by incorporating a few mol% of *N*-methyl-*N*-(4-  
15  
16 vinylphenethyl)ethylenediamine (MVEDA) into HEMA. In one of his last publications, Professor  
17  
18 Tsuruta<sup>25</sup> postulated a mechanism on the suppression. That is, the introduction of extraneous  
19  
20 comonomers would loosen the intermolecular hydrogen-bonding network of PHEMA and allow  
21  
22 water molecules to readily infiltrate into the polymer matrix; so that makes the PHEMA chains as  
23  
24 well as water molecules more mobile to form the soft biological surface, where *IW* predominates  
25  
26 and blood compatibility increases. This suggestion encouraged Tanaka et al.<sup>26</sup> to push their  
27  
28 research employing small amounts of comonomers, not only in HEMA<sup>27 28 29</sup> but also in MEA  
29  
30 polymers,<sup>30</sup> in order to understand the contribution of such monomers to increasing the bio-inert  
31  
32 properties of the copolymers. In addition to introducing nitrogen atoms (MVEDA contains amino  
33  
34 groups), a variety of elements have been incorporated into HEMA copolymers and their  
35  
36 contribution to bio-inert properties was investigated. Zhao et al.<sup>31</sup> investigated the adsorption  
37  
38 behavior of bovine serum albumin (BSA) and human plasma fibrinogen (HFg) using the surface  
39  
40 coated by poly(2-perfluorooctylethyl methacrylate (FMA)-*co*-HEMA). The adsorption behavior  
41  
42 on FMA-*co*-HEMA copolymer depends on the type of protein, the lowest adsorption amount of  
43  
44 BSA and HFg were observed with 7.56 and 2.45 mol% of FMA loading, respectively.

45  
46  
47 Furthermore, there are reports on random<sup>27</sup>, block<sup>28</sup> and graft<sup>29</sup> copolymers of HEMA with MEA;  
48  
49 the protein-fouling resistance enhancement was also detected by incorporating a small amount of  
50  
51

1  
2  
3 MEA into HEMA. Although there was no significant difference in the number of adhered platelets,  
4  
5 the largest amount of *IW* was expressed when HEMA content was 20 mol% for the random, 9.6  
6  
7 mol % for the block, and 40 mol% for the graft copolymers of HEMA and MEA. Recently, we  
8  
9 reported MEA copolymers containing small amount of 2,2,2-trifluoroethyl methacrylate  
10  
11 (TFEMA), in which the IWC was increased and the copolymers showed improved bio-inert  
12  
13 properties.<sup>30</sup> These results suggest that controlling the chemical structure of polymer leads to  
14  
15 control of the hydration structure. Therefore, in this study, we dared to select non-bio-inert  
16  
17 comonomers for the syntheses of HEMA copolymers and evaluated the bio-inertness to examine  
18  
19 the above hypothesis. Whitesides et al.<sup>32 33</sup> reported that surfaces which resist protein adsorption  
20  
21 have the following characteristics: 1) they are hydrophilic; 2) they do not contain hydrogen-bond  
22  
23 donors but hydrogen-bond acceptors; 3) they are overall electrically neutral.

24  
25  
26  
27  
28  
29 One of the monomers we chose is an amino-functionalized monomer, 2-(dimethylamino)ethyl  
30  
31 methacrylate (DMAEMA) which has a -NCH<sub>3</sub> group. The pKa of its polymer was reported to be  
32  
33 8.4 and more than 90% becomes cationic under the physiological environment.<sup>34</sup> In addition,  
34  
35 polyDMAEMA is one of the well-known biomaterials used as non-viral gene delivery vectors.<sup>35,36</sup>

36  
37  
38  
39 Another one is fluorine-containing monomer, TFEMA. We have already reported the bio-  
40  
41 incompatibility of the obtained polymer, PTFEMA-coated substrate exhibited the water in air  
42  
43 contact angle of 96.9 degrees, and it displayed a very high degree of fibrinogen adsorption and  
44  
45 denaturation as well as a large number of adhered platelets.<sup>30</sup> This monomer is also classified as a  
46  
47 non-bioinert monomer that deviates from the above-mentioned property of hydrophilic. Notably,  
48  
49 the homopolymer PTFEMA is soluble in non-fluorine solvent such as DMF and the hydrophilic  
50  
51 PHEMA is also soluble in DMF; the characteristic solubility of PTFEMA leads us to obtain the  
52  
53  
54  
55  
56  
57  
58  
59  
60

1  
2  
3 amphiphilic copolymers. It is therefore expected that TFEMA can be copolymerized with  
4  
5 hydrophilic HEMA to give a copolymer with a composition that reflects the feed monomer ratio.  
6  
7

8  
9 In this work, we synthesized HEMA binary and ternary copolymers containing small  
10  
11  
12 amounts of DMAEMA, TFEMA, and a combination of both monomers to evaluate their  
13  
14  
15 responses to proteins and platelets. We discuss the expression mechanisms of bioinert  
16  
17  
18  
19 properties on the copolymers in terms of their hydration states.  
20  
21  
22  
23  
24  
25  
26  
27  
28  
29  
30  
31  
32  
33  
34  
35  
36  
37  
38  
39  
40  
41  
42  
43  
44  
45  
46  
47  
48  
49  
50  
51  
52  
53  
54  
55  
56  
57  
58  
59  
60

## Experimental section

### Experimental Part

#### 1. Materials

HEMA, DMAEMA, and TFEMA (all from TCI chemicals) were used as received without further purification. All other solvents and chemicals were used as received unless otherwise stated.

#### 2. Synthesis of the HEMA copolymers

The HEMA copolymers were synthesized by performing free radical homo- and copolymerizations of HEMA with DMAEMA and TFEMA. The molar ratios of HEMA to DMAEMA and TFEMA are shown in Table 1. The following describes the reaction conditions with a ratio of 80:10:10 as a representative example. To a pressure glass vessel, 1.70 mL of HEMA (80 mmol), 0.95 mL of DMAEMA (10 mmol), 0.249 mL of TFEMA (10 mmol), 11.88 mL of DMF, and 24.0 mg of 2,2'-azobis(isobutyronitrile) (AIBN, 0.15 mmol) as an initiator were added, nitrogen was purged to eliminate the air, and the reaction was conducted at 80 °C for 15 hours. The copolymer was obtained as a white solid precipitate, by pouring the DMF solution to diethyl ether. After decantation, the precipitate was dissolved in ethanol, precipitated in hexane for purification, and dried at 40 °C under reduced pressure.

#### 3. Analyses.

##### 3-1) Characterization of the chemical structure of obtained polymers

1  
2  
3 The HEMA copolymers were characterized by  $^1\text{H}$  NMR, using a JEOL 500 MHz JNM-ECX  
4 spectrometer at room temperature in DMSO- $d_6$  as the solvent. The chemical shifts are reported in  
5  $\delta$  ppm downfield from TMS.  
6  
7

8  
9  
10 Molecular weights were determined by gel permeation chromatography (GPC) employing an  
11 integrated SEC unit of a Tosoh HLC-8320 chromatograph equipped with three Styragel HR  
12 columns connected in series (WAT044229, WAT044241, and WAT044235) and a refractive  
13 index (RI) detector. Measurements were performed with DMF as an eluent, containing 10 mM  
14 lithium bromide at 40 °C with a 1.0 mL/min flow. Molecular weights were calculated using PEG  
15 standards with narrow molecular weight distribution in the range of  $1.96 \times 10^3 - 1.02 \times 10^6$  g/mol.  
16  
17  
18  
19  
20  
21  
22  
23  
24  
25  
26  
27  
28

### 29 **3-2) Thermal property evaluation and quantification of the interactions between water and** 30 **(co)polymers.** 31

32  
33  
34 Differential Scanning Calorimetry (DSC) measurements were executed using Q1000  
35 from TA Instruments in a temperature range of  $-80$  to  $100$  °C at a heating rate of  $5$  °C  
36  $\text{min}^{-1}$  under nitrogen. Dry  $T_g$  was determined automatically by the instrument from the  
37 second heating trace and is reported as the midpoint of the thermal transition. The  
38 hydrated  $T_g$  was defined by the peak position of DDSC that is temperature derivative of  
39 DSC during the heating process. The preparation of hydrated sample and the analysis of  
40 the amount of hydration water in the hydrated polymers were performed with a previously  
41  
42  
43  
44  
45  
46  
47  
48  
49  
50  
51  
52  
53  
54  
55  
56  
57  
58  
59  
60

1  
2  
3 reported method.<sup>14</sup> The hydrated samples were prepared by immersing in ultrapure water for  
4  
5  
6 more than 3 days before performing the measurements.  
7

8  
9 Based on the interactions of water molecules with the polymer chains, we classified three types  
10 of water in hydrated polymers; non-freezing water (*NFW*), intermediate water (*IW*), and free water  
11 (*FW*) those are tightly, loosely, and scarcely bound to the polymer, respectively. Their  
12 content is given as *NFWC*, *IWC*, and *FWC*, respectively. The DSC measurements ~~was~~ were  
13 performed with 3 to 7 mg weight of the samples. The sample weight was checked before and after  
14 the DSC measurement to ensure the proper seal of the sample pan. The data from samples with  
15 weight change were omitted.  
16  
17

18 The water content of the polymer was adjusted by changing the drying time and temperature  
19 before sealing. Under the applied measurement's conditions, pure water shows a sharp exothermic  
20 peak at about -18 °C in the cooling process on the DSC thermogram and an endothermic peak at  
21 about 1 °C in the heating process. The maximum water content at which these peaks do not appear  
22 was defined as equilibrium water content (*EWC*), and is given by the following Equation (1):  
23  
24

$$25 \text{ EWC (wt\%)} = ((W_1 - W_0) / W_1) \times 100 \quad (1)$$

26 where  $W_0$  and  $W_1$  are the weights of the dry and hydrated samples, respectively.  
27  
28

29 The amounts of the different types of water in the hydrated polymers are given by the following  
30 Equations:  
31  
32

$$33 \text{ EWC (wt\%)} = \text{NFW (wt\%)} + \text{IW (wt\%)} + \text{FW (wt\%)} \quad (2)$$

$$34 \text{ IW (wt\%)} = \Delta H_{cc} / 334(\text{Jg}^{-1}) \quad (3)$$

$$35 \text{ FW (wt\%)} = (\Delta H_m / 334(\text{Jg}^{-1})) - \text{IW} \quad (4)$$

1  
2  
3  $\Delta H_{cc}$  and  $\Delta H_m$  are enthalpy changes during cold crystallization and the melting of ice,  
4  
5 respectively.  
6  
7  
8  
9

### 10 11 **3-3) Quantification of the mobility of the polymers in the hydrated state**

12  
13  
14 Water mobility at the hydrated state of the polymers was quantified by a low-field NMR  
15 spectrometer (Bruker Minispec mq20) at 20 MHz using  $^1\text{H}$  NMR. Spin-spin relaxation time ( $T_2$ )  
16 was measured using a Carr-Purcell-Meiboom-Gill (CPMG) pulse sequence at 40 °C.  
17  
18 Approximately 400 mg of the samples were used. The hydrated samples were prepared by  
19 immersing in ultrapure water for more than 3 days before measurements. The presence of the two  
20 types of water molecules, interacting or non-interacting water molecules, can be reproduced using  
21 a linear combination of a following exponential Equation (5):<sup>37</sup>  
22  
23  
24  
25  
26  
27  
28  
29  
30

$$31 \exp(-t / T_2) = a \exp(-t / T_{2 \text{ interacting water}}) + b \exp(-t / T_{2 \text{ non-interacting water}}) \quad (5),$$

32  
33  
34 where the corresponding weight ratio,  $a$  and  $b$  are normalized as  $a + b = 1$ . In this case,  
35  
36 interacting water consists of  $NFW$ ,  $IW$ , and  $FW$ . To evaluate  $T_{2 \text{ interacting water}}$ ,  $a$  (that is the weight ratio  
37 of the interacting water, equal to EWC) was determined from the DSC measurement.  $T_{2 \text{ non-interacting}}$   
38  
39 water was determined by conducting the same experiment for water only.  $b$  was calculated after  
40  
41 drying the sample used for the DSC measurement.  
42  
43  
44  
45  
46  
47  
48  
49

### 50 **3-3) Preparation and characterization of the polymer surfaces**

51  
52  
53 Film samples were prepared as follows and were used for contact angle (CA), X-ray  
54 photoelectron spectroscopy (XPS) measurement, and the human blood platelet adhesion test. The  
55  
56  
57  
58  
59  
60

1  
2  
3 polymer samples were dissolved in ethanol or methanol to prepare a 0.2 wt /vol % solution and  
4  
5 filtered. The solution was spin-coated onto round-shaped 14 mm  $\phi$  substrates that was washed by  
6  
7 methanol prior to coat the surface. The substrates were coated twice with the solution using a  
8  
9 Mikasa spin coater MS-A100 at rates of 500 rpm for 5 s, 2000 rpm for 10 s, slope for 5 s, 4000  
10  
11 rpm for 5 s, and slope for 4 s; and then the substrates were dried at room temperature.  
12  
13  
14

15 CA of water on the polymer coated surface was measured at 25 °C by the sessile drop method.  
16  
17 The captive bubble method was used to evaluate the hydrated surface. 2  $\mu$ L of air bubbles are  
18  
19 injected beneath the hydrated surface immersed in water.<sup>14,15,16,30</sup> The reported values for both  
20  
21 measurements are the average of three measurements made at different positions of the substrate.  
22  
23  
24

25 XPS measurement was carried out on an ESCA-5500 (Physical Electronics, Inc.)  
26  
27 equipped with a monochromated Al K $\alpha$  X-ray source. The measurements were performed  
28  
29 at a photoelectron take-off angle (measured with respect to the plane of the sample) of  
30  
31 45 degrees to the polymer-coated substrates. Charge compensation was achieved with  
32  
33 a low energy electron flood gun.  
34  
35  
36  
37  
38  
39  
40  
41  
42  
43  
44  
45  
46

### 47 **3-4) Protein Adsorption and Deformation evaluation by micro BCA and ELISA**

48

49 The micro BCA was performed in order to measure the amount of adsorbed proteins on the  
50  
51 polymer surfaces. Fibrinogen (Sigma) was used as the protein, and the analyses were performed  
52  
53 as published before.<sup>14,15,16,30</sup> ELISA was executed to determine the amount of the exposed gamma  
54  
55  
56  
57  
58  
59  
60



1  
2  
3 chains in fibrinogen. The polymer surfaces were prepared for both micro BCA and ELISA by the  
4 following manner: 100  $\mu\text{L}$  of the polymer solution (0.2 wt /vol%) in ethanol was added to the  
5  
6 polypropylene (PP) 96-well plate. The plate was slowly air-dried over 3 days at room temperature.  
7  
8  
9

10 Two types of polymer-casted 96-well PP plates were prepared. One is the water pre-soaked  
11 (priming) substrate, which was immersed in 200  $\mu\text{L}$  PBS for 16 hours at 37  $^{\circ}\text{C}$ , and after that the  
12  
13 PBS was removed. The other is the non-priming substrate that was not subjected to PBS prior to  
14  
15 perform micro BCA and ELISA analyses.  
16  
17  
18  
19  
20  
21  
22  
23  
24

### 25 **3-5) Preparation of Polymer Substrates and Human Platelet Adhesion Test**

26  
27 The polymer substrates used in the human platelet adhesion tests were prepared as follows: The  
28 polymer-coated substrates were cut into 8  $\times$  8 mm squares. The substrates were then fixed on an  
29  
30 Scanning Electron Microscope (SEM) specimen stage using double-sided tape. Platelet-rich  
31  
32 plasma (PRP) and platelet-poor plasma (PPP) were obtained from human blood by two stages of  
33  
34 centrifuging.<sup>14,15,16,30</sup>  
35  
36  
37  
38  
39

40 SEM was used to quantify the number of platelets adhered to the substrates. For statistical  
41 purposes, the platelet adhesion test was performed three times with human blood from different  
42  
43 donors. The reported values are the average of 5 measured points on 3 different films, excluding  
44  
45 the maximum and the minimum value.  
46  
47  
48  
49  
50  
51  
52

### 53 **3-6) Statistical analysis**

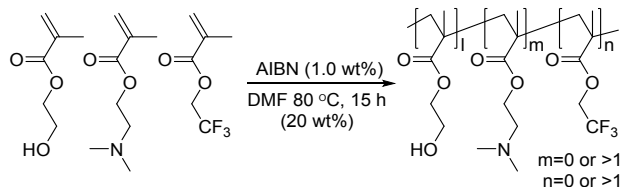
54  
55  
56  
57  
58  
59  
60

1  
2  
3 All the data are expressed as means  $\pm$  SD. The significance of the differences between  
4  
5  
6  
7 two samples was determined using an unpaired Student's t-test using Microsoft Excel  
8  
9  
10  
11 2013. Differences with P values less than 0.05 were statistically significant.  
12  
13  
14  
15  
16  
17  
18  
19  
20  
21  
22  
23  
24  
25  
26  
27  
28  
29  
30  
31  
32  
33  
34  
35  
36  
37  
38  
39  
40  
41  
42  
43  
44  
45  
46  
47  
48  
49  
50  
51  
52  
53  
54  
55  
56  
57  
58  
59  
60

## Results and Discussion

HEMA copolymers were prepared using either one or both of the comonomers DMAEMA and TFEMA. The synthetic route is outlined in Scheme 1.

### Scheme 1. Synthetic route to HEMA copolymers



### 1. Synthesis and characterization of the HEMA copolymers

Binary and ternary copolymers were synthesized as shown in Scheme 1: poly(HEMA-*co*-DMAEMA) (N-series), poly(HEMA-*co*-TFEMA) (F-series), and poly(HEMA-*co*-DMAEMA-*co*-TFEMA) (N&F-series).

The composition of copolymers was estimated by  $^1\text{H}$  NMR analysis of the peak for  $-\text{OH}$  in HEMA at  $\delta$  4.80 ppm,  $-\text{CH}_2-\text{N}(\text{CH}_3)_2$  in DMAEMA at  $\delta$  3.30 ppm, and  $-\text{O}-\text{CH}_2-\text{CF}_3$  in TFEMA at  $\delta$  4.30 ppm (Figure S1). The monomer composition shown in Table 1 is in good agreement with the monomer ratio in the reaction mixture. PDMAEMA shows high water solubility and this property can be imparted to the HEMA copolymers by copolymerizing 50 or more mol% of DMAEMA. The molecular weight and molecular weight distribution of all polymers are very similar. Figure S2 shows the GPC data of all polymers. The GPC trace of PHEMA has a shoulder at the low MW region, and all HEMA copolymers possess this characteristic. Additionally, higher amount incorporation of DMAEMA (in N10 and N25) cause a shoulder in the high MW region. The RI of fluorine is low and close to that of DMF, and therefore F50 and F100 showed weak intensity peaks despite the same concentration.

**Table 1.** Composition, yield, and the molecular weight characteristics of all the synthesized HEMA copolymers.

Category	Code	Mol. ratio (l/m/n)		Yield (%)	$M_n^b$ (g/mol)	$M_w/M_n^b$
		Feed	Found <sup>a</sup>			
Control	PHEMA	100 / 0 / 0	100 / 0 / 0	79.5	14500	2.44
N-series	N1	99 / 1 / 0	99 / 1 / 0	94.9	18700	2.02
	N3	97 / 3 / 0	97 / 3 / 0	80.3	15600	2.44
	N5	95 / 5 / 0	95 / 5 / 0	84.3	15500	2.08
	N7	93 / 7 / 0	93 / 7 / 0	90.7	15500	1.92
	N10	90 / 10 / 0	90 / 10 / 0	89.7	14600	3.26
	N25	75 / 25 / 0	75 / 25 / 0	68.8	15500	4.90
	N100	0 / 100 / 0	0 / 100 / 0	33.4	27300	1.26
F-series	F1	99 / 0 / 1	99 / 0 / 1	91.6	19400	2.04
	F3	97 / 0 / 3	97 / 0 / 3	89.3	17400	2.28
	F5	95 / 0 / 5	95 / 0 / 5	94.7	17300	2.44
	F7	93 / 0 / 7	93 / 0 / 7	75.4	17100	2.22
	F9	90 / 0 / 10	91 / 0 / 9	88.2	16500	2.32
	F26	75 / 0 / 25	74 / 0 / 26	80.6	17500	2.07
	F100	0 / 0 / 100	0 / 0 / 100	68.5	10200	1.71

N&F -series	N3F4	94 / 3 / 3	93 / 3 / 4	97.5	18200	2.29
	N5F5	90 / 5 / 5	90 / 5 / 5	99.8	18000	2.20
	N7F8	86 / 7 / 7	85 / 7 / 8	85.3	15200	2.54
	N10F10	80 / 10 / 10	80 / 10 / 10	89.1	15200	2.75

<sup>a</sup> The copolymer composition was identified by <sup>1</sup>H-NMR. <sup>b</sup> Molecular weight was measured by GPC carried out in DMF using PEGs as standards.

## 2. Protein adsorption/denaturation behavior on the surface of HEMA copolymers.

Figure 1 summarizes the results of fibrinogen adsorption and the exposure degree of the gamma chain of fibrinogen. The synthesized N-series and F-series were coated on 96 well plate, and the surface was analyzed for the samples with or without priming. The values showed the minimum in both adsorption amount and denaturation degree when a small amount (3-10 mol%) of the comonomer was incorporated. Although the chemical structure is different from the comonomers in this work, a similar trend was reported for HEMA copolymers with MVEDA<sup>24</sup> and FMA.<sup>31</sup> It is safely assumed that there is an optimal copolymer composition to achieve high bio-inert properties in HEMA copolymers. Since

this trend appeared to be more pronounced with substrate priming, the hydration structure of the copolymers was further investigated using DSC.

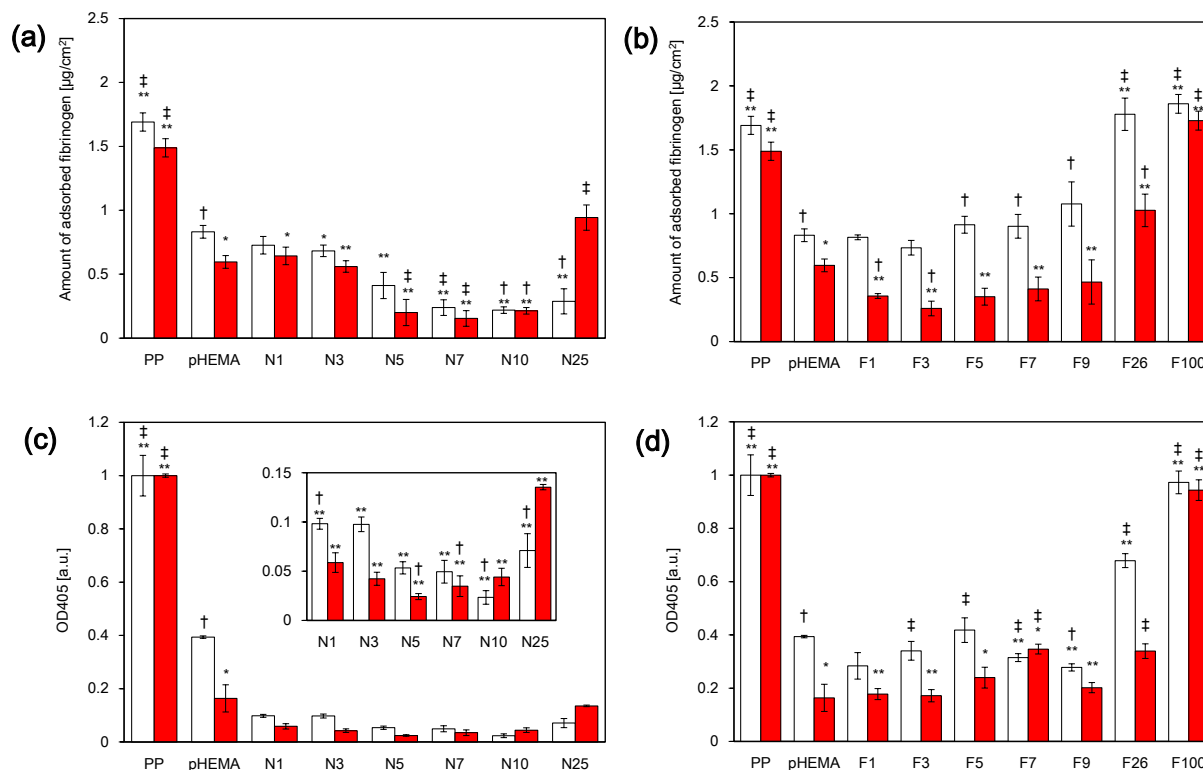


**Figure 1.** The amount of fibrinogen adsorption (a, b), the exposure of gamma chain of fibrinogen (c, d) onto the surfaces of HEMA copolymers using without (white bar) and with priming (red bar). PP is included as control surface. The inset in (c) is an enlarged graph for N1 to N25. The data represent the means  $\pm$  SD ( $n = 3$ ) of fibrinogen adsorption and denaturation \*:  $P < 0.05$ , \*\*:  $P < 0.01$  vs. PHEMA without priming and †:  $P < 0.05$ , ‡:  $P < 0.01$  vs. PHEMA with priming substrate.

### 3. Hydration characteristics of HEMA copolymers

#### 3-1) Analysis of the hydration structure by DSC.

The hydration structure was evaluated by DSC, and the water content relative to the comonomer composition was summarized in Figure 2. Detailed evaluation results for both N- and F-series, and the DSC profiles at the EWC and different water content are in supporting information (see Table S1 and Figure S3-S20). Biomolecules such as proteins and platelets interact with materials in the aqueous medium, so it can be considered that they are interacting with each other under EWC conditions. Therefore, quantification of EWC is important to consider the interaction between these molecules. The EWC was found to increase with DMAEMA and decreased with TFEMA, depending on the type and amount of comonomer. It deems that the variation of EWC is brought about by the characteristics of each comonomer that are more hydrophilic or hydrophobic than HEMA. Additionally, EWC was roughly additive and correlated with the composition of the copolymerized monomers. However, each water content was not changed additively in

the range up to about 10 mol%. The N-series showed a decrease in *NFW* despite an increase in *EWC*. On the other hand, although the F-series maintained a certain amount of *NFW*, *FW* decreased more rapidly than *EWC*.

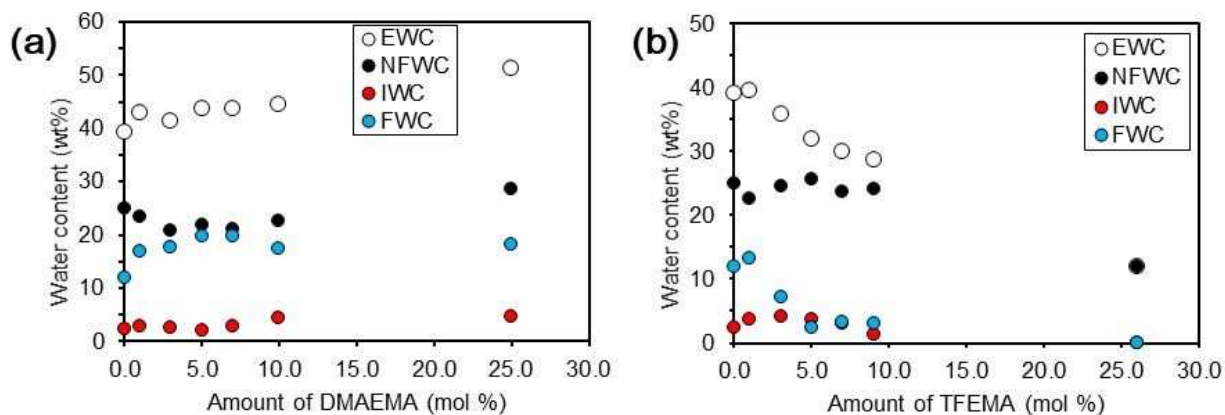


**Figure 2** Dependence of the water content on the amount of the introduced DMAEMA (a) and TFEMA (b) at EWC.

### 3-2) Molecular mobility analysis in hydrated state by DDSC.

Since PHEMA has a -OH group in the side chain, it can form a hydrogen-bonding network through intra- and inter-molecular interactions. Therefore, PHEMA exhibits a higher  $T_g$  than that of poly(propyl methacrylate) with a similar side chain length. Morita et al.<sup>38</sup> investigated the hydrogen-bonding structure in PHEMA by infrared spectroscopy, and OH  $\cdots$  O=C and OH  $\cdots$  OH types of hydrogen bonds were observed. Table 2 shows  $T_g$  of synthesized polymers for both



1  
2  
3 experimental and predicted values. Fox's equation was used to calculate the predicted values, the  
4  
5 reciprocal of the copolymer's  $T_g$  is given by the sum of the reciprocal of each homopolymer's  $T_g$   
6  
7 multiplied by its weight fraction. However, as can be seen from Table 2, N10 and F26 showed  
8  
9 almost the same  $T_g$  as PHEMA. Furthermore, the value was almost constant regardless of the  
10  
11 comonomer content. Thus, the incorporation of a small amount of comonomer into PHEMA is not  
12  
13 sufficient to break-up the hydrogen bonding network in the dry state (For DSC thermograms, see  
14  
15 Figure S21 in supporting information).  
16  
17  
18

19  
20 In general, plasticizers are known to work by weakening the polymer-polymer interaction  
21  
22 and thus reduce the  $T_g$  of polymers. Water molecules sorbed into PHEMA interact  
23  
24 strongly with hydroxy group at the side chain termini and exhibit plasticizing effect by  
25  
26 disrupting the hydrogen-bonding polymer network. Consequently, the molecular mobility  
27  
28 of PHEMA drastically changed upon hydration and the high mobility of polymer chain can  
29  
30 be observed as a  $T_g$  reduction on DSC thermogram. Hatakeyama et al.<sup>39</sup> reported the  
31  
32 estimation of  $T_g$  for a copolymer of styrene and 4-hydroxystyrene using Fox's equation.  
33  
34 Additionally, they also reported that when a small amount of water molecules is present, the  
35  
36 hydroxyl groups in the polymer interact with water to break the inter-/intra-polymer hydrogen  
37  
38 bonding. Further increase of the water content plasticizes the polymer additionally.<sup>40</sup>  
39  
40  
41  
42  
43  
44  
45  
46  
47  
48  
49  
50

51  
52 Meakin et al.<sup>41</sup> reported that the  $T_g$  of PHEMA dropped to about 50 °C from 113 °C by about 8  
53  
54 wt% hydration from the dry state. They estimated the  $T_g$  of hydrated PHEMA by applying the  
55  
56  
57  
58  
59  
60

1  
2  
3  
4 Fox's equation with their EWC,  $-136\text{ }^{\circ}\text{C}$  was used as the  $T_g$  of water.<sup>42</sup> Kim et al.<sup>43</sup> calculated  
5  
6  
7 the hydrated  $T_g$  of Nafion by substituting EWC into the Kelley-Bueche Equation,<sup>44</sup> which  
8  
9  
10 was in a good agreement with the observed  $T_g$  at low water content, but not at high water  
11  
12  
13 content. From this result, the authors concluded that freezable water molecules, which  
14  
15  
16 crystallize at temperatures higher than  $-80\text{ }^{\circ}\text{C}$ , do not significantly affect  $T_g$  in hydrated  
17  
18  
19 state. Tran et al.<sup>45</sup> also reported estimations for the hydrated  $T_g$  of polyethylene glycol diacrylate  
20  
21  
22 copolymers with poly(ethylene glycol) methyl ether acrylate, sulfobetaine methacrylate, 2-  
23  
24 acrylamido-2-methyl-1-propanesulfonate sodium, and [2-(acryloyloxy)ethyl] trimethyl  
25  
26 ammonium chloride. The estimation showed good agreements with the observed  $T_g$  by using the  
27  
28  
29 NFWC rather than EWC.  
30  
31  
32  
33  
34

35 Since the  $T_g$  of HEMA copolymers in the hydrated state was difficult to observe by DSC clearly,  
36  
37 the peak top of DDSC in the heating scan was used as the  $T_g$ . The DDSC curve for the N- and F-  
38  
39 series polymers are shown in Figure 3. For the F-series copolymers with more than 7 mol%  
40  
41 TFEMA, no apparent  $T_g$  was observed in DDSC. From the  $\Delta^{\text{NFWC}}$  in Table 2, the hydrated  $T_g$  tends  
42  
43 to be predicted as  $10\text{ }^{\circ}\text{C}$  lower than the observed value. We are now speculating that the DDSC  
44  
45 peaks of F7 and F9 were overlapped with the endothermic peaks of ice-melting at about  $0\text{ }^{\circ}\text{C}$   
46  
47 because the hydrated  $T_g$  tends to be predicted at  $10\text{ }^{\circ}\text{C}$  lower as in the case of a fluorine amount  
48  
49 less than in F5. Additionally, the DDSC peaks for F26 and F100 were predicted to appear at above  
50  
51  
52  $30\text{ }^{\circ}\text{C}$ , and were not detected below  $50\text{ }^{\circ}\text{C}$ .  
53  
54  
55  
56  
57  
58  
59  
60

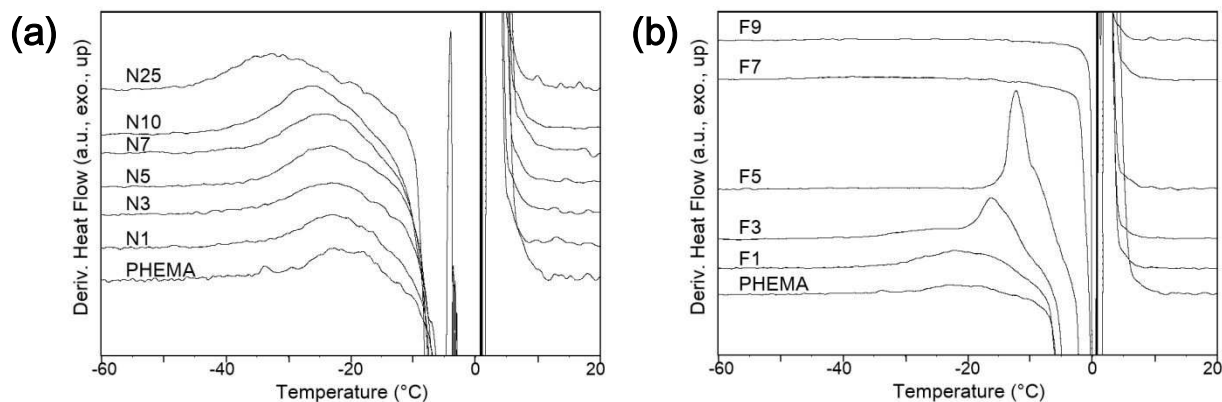


**Figure 3.** Analyses of hydrated  $T_g$  of N-series (a) and F-series (b) by DDSC.

The measured dry and hydrated  $T_g$ s will be further discussed together with the theoretical values estimated from Fox's equation. These values are presented in Table 2 and the hydrated  $T_g$  is calculated from EWC and NFWC. The value for the hydrated  $T_g$  is found to be closer to that of the experimental values when using NFWC instead of EWC as the interacting water fraction. These results indicate that only strongly bound water, *NFW*, acts to disrupt the stable hydrogen bonding network in PHEMA, while freezable *IW* and *FW* molecules do not affect plasticization and  $T_g$  reduction.

**Table 2**  $T_g$ 's from actual DSC measurements and calculated by the Fox equation

Category	Code	Dry $T_g$ (°C)			Hydrated $T_g$ (°C)				
		Observed	Predicted <sup>a</sup>	$\Delta$ Dry <sup>b</sup>	Observed	Predicted <sup>EWC c</sup>	$\Delta$ EWC <sup>d</sup>	Predicted <sup>NFWC e</sup>	$\Delta$ NFWC <sup>f</sup>
Control	PHEMA	94.6	94.6	0.0	-22.7	-54.6	31.9	-29.0	6.3
N-series	N1	93.5	93.4	0.1	-23.3	-63.1	39.8	-29.3	6.0
	N3	93.3	91.2	2.1	-23.6	-59.5	35.9	-21.3	-2.3
	N5	94.0	88.9	5.1	-20.2	-64.5	44.3	-26.2	6.0
	N7	94.0	86.7	7.2	-24.3	-64.3	40.0	-23.6	-0.7
	N10	96.8	83.5	13.3	-26.8	-65.4	38.6	-27.7	0.9
	N25	90.9	68.9	22.0	-32.6	-79.3	46.7	-50.0	17.4
	N100	18.3	18.3	0.0	- g	- g	- g	- g	- g
F-series	F1	94.4	94.5	0.0	-22.3	-55.6	33.3	-24.0	1.7
	F3	93.8	94.2	-0.4	-17.2	-47.1	29.9	-25.3	8.1
	F5	96.0	93.9	2.1	-12.3	-36.4	24.1	-23.6	11.3

	F7	90.7	93.6	-2.9	- <sup>h</sup>	-32.5	- <sup>h</sup>	-19.2	- <sup>h</sup>
	F9	95.4	93.3	2.1	- <sup>h</sup>	-27.7	- <sup>h</sup>	-17.7	- <sup>h</sup>
	F26	94.5	91.1	3.4	- <sup>h</sup>	30.8	- <sup>h</sup>	30.8	- <sup>h</sup>
	F100	83.6	83.6	0.0	- <sup>h</sup>	74.4	- <sup>h</sup>	74.4	- <sup>h</sup>

<sup>a</sup> Estimated from the Fox's equation. <sup>b</sup> $\Delta^{Dry}$  defined as dry  $T_g$  (Observed) –dry  $T_g$ .(Predicted). <sup>c</sup> Estimated from the Fox's equation by using EWC as the water content. <sup>d</sup>  $\Delta^{EWC}$  defined as hydrated  $T_g$  (Observed) –hydrated  $T_g$ .(Predicted<sup>EWC</sup>). <sup>e</sup> Estimated from the Fox's equation by using the NFWC as the water content. <sup>f</sup>  $\Delta^{NFWC}$  defined as hydrated  $T_g$  (Observed) –hydrated  $T_g$ .(Predicted<sup>NFWC</sup>). <sup>g</sup> Not defined as water soluble. <sup>h</sup> Not detected clear peak below 50 ° C.

### 3-3) Analysis of water mobility by solid-state $^1\text{H}$ pulse NMR.

The water molecules in a polymer matrix also change their mobility by molecular interaction with polymer chains. According to the Bloembergen-Purcell-Pound theory,<sup>46,47</sup> the spin-spin relaxation time,  $T_2$ , decreases continuously as the correlation time,  $\tau_c$ , increases. Tanzawa<sup>48</sup> roughly classified the water molecules into three types based on the difference in  $\tau_c$  of  $10^{-6}$  sec,  $10^{-9}$  sec, and  $10^{-11}$  sec, as *NFW*, *IW*, and *FW*, respectively - the longer the  $T_2$  of water, the higher the mobility. In other words, the mobility of water decreases by interacting with the polymer, and  $T_2$  decreases. The  $T_2$  of water was measured by solid-state  $^1\text{H}$  pulse NMR<sup>43</sup> using hydrated samples with water content close to their EWC quantified by DSC. The results are presented in Figure 4, together with the hydrated  $T_g$  of the materials.

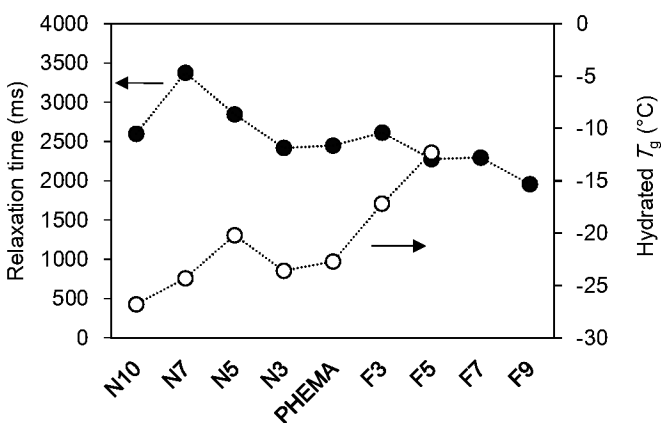


**Figure 4.** Relaxation time of water and hydrated  $T_g$  of the HEMA copolymers.

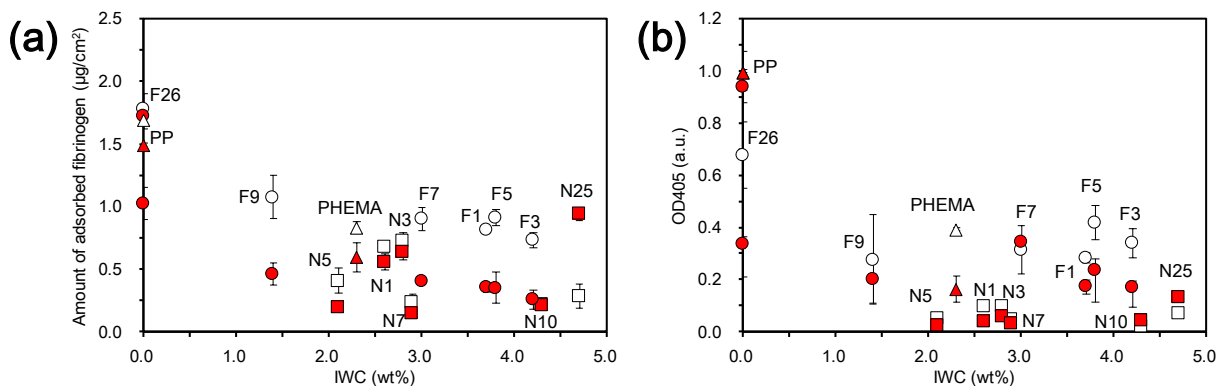
1  
2  
3 Compared to hydrated homo- PHEMA, the relaxation time of water in copolymers with a small  
4 amount of foreign elements (N or F) was decreased with the introduction of TFEMA, and increased  
5 with DMAEMA. The relaxation time of pure water was found to be about 3100 msec, close to the  
6 previously reported value of 3195 msec ( $1/T_2 = 0.313 \text{ sec}^{-1}$ ).<sup>49</sup> Relaxation spectra of water in all  
7 (co)polymers are shown in Figure S22 (see supporting information).  
8  
9  
10  
11  
12  
13  
14  
15  
16

17 Considering the result of  $T_2$  analysis together with the result of the hydrated structure analysis by  
18 DSC (Figure 2), by copolymerizing small amounts of foreign monomers with HEMA, the  
19 following changes in hydration state can be caused by the changes in intra- and inter- molecular  
20 interactions. Introducing a small amount of DMAEMA into HEMA copolymers reduces the  
21 amount of hydroxyl groups that can strongly interact with the hydrogen-bonding site. This  
22 reduction in hydroxy groups reduces the interaction between polymer chains; thus the free volume  
23 increases. Furthermore, since the number of functional groups that have a role in polymer-water  
24 interaction is reduced, resulting in an increase in  $IW$  and  $FW$  with less interaction with the polymer.  
25  
26 As a result, the strong hydrogen-bonding network of water due to the interaction between water  
27 and PHEMA is loosened, and a part of  $NFW$  changes to  $IW$  or  $FW$ . However, when the DMAEMA  
28 composition is as high as 50 mol%, the polymer became water-soluble because of the  
29 predominance of the interaction between water and  $-NCH_3$ . Conversely, by introducing a small  
30 amount of TFEMA into HEMA copolymers, the hydrophobic fluorine groups are agglomerated  
31 due to hydrophobic interaction upon the hydration of PHEMA matrix. This aggregate acts as a  
32 physical cross-linking point, thereby reducing the free volume, and consequently increasing  $NFW$   
33 that strongly interacts with the polymer. Fluorinated side chains are highly hydrophobic and  
34  
35  
36  
37  
38  
39  
40  
41  
42  
43  
44  
45  
46  
47  
48  
49  
50  
51  
52  
53  
54  
55  
56  
57  
58  
59  
60

1  
2  
3 their affinity with water is weak. Therefore, it can also be interpreted that  $T_g$ , the  
4  
5  
6  
7 temperature at which micro Brownian motion of polymer starts, was increased by the  
8  
9  
10 promotion of dehydration from the polymer chains. Thus, the stable network between water  
11  
12  
13 and PHEMA gets stronger, and a part of  $FW$  changes to  $IW$  and  $NFW$ .

#### 4. Relationship between hydration structure and biological response

20  
21  
22 The relationship between the fibrinogen adsorption/denaturation to the hydration state is  
23  
24  
25 shown in Figure 5. The comonomer composition is also shown in the figure. The role of  
26  
27  
28  
29  
30  $IW$  is interpreted to shield the blood component from direct contact with  $NFW$ , and it has  
31  
32  
33 been reported that the blood component is not activated if a sufficiently thick  $IW$  is  
34  
35  
36 present.<sup>50</sup> Therefore here, IWC is used as an index of the hydration structure.





1  
2  
3 **Figure 5.** Correlation between the ratio of IWC and the biological response: fibrinogen  
4  
5  
6 adsorption (a), and the exposure of gamma chain of fibrinogen (b). The data represent the means  
7  
8  $\pm$  SD (n = 3). PP is included as control surface. Squares, circles, and triangles indicate N-series, F-  
9  
10 series, and controls, respectively, and white and red indicate without and with priming,  
11  
12 respectively.  
13  
14  
15

16  
17  
18  
19 As can be seen in Figure 5, the substrates coated with the HEMA copolymers showed lower  
20  
21 fibrinogen adsorption and denaturation as the content of IWC increases. In particular, this trend  
22  
23 became more prominent with priming, and the relationship between IWC and the biological  
24  
25 response is in good agreement with previous works.<sup>14,30</sup> However, although IWC of F9 was about  
26  
27 half that of N25, the amount of adsorbed fibrinogen was less than half. This discrepancy seems to  
28  
29 be due to the surface hydration structure; thus the surface was therefore further investigated by  
30  
31 contact angle and XPS measurements.  
32  
33  
34  
35

### 36 **5. Contact angle measurements of dry and hydrated HEMA copolymer films**

37

38  
39 The water in air contact angles (WCA, sessile drop method) and the air in water contact angles  
40  
41 (ACA, captive bubble method) of the HEMA copolymers are summarized in Table 3. The WCA  
42  
43 results show that the contact angle of sessile drop changes over time. Immediately after the water  
44  
45 droplet contact with the surface, WCA of the copolymers is higher than homo- PHEMA in most  
46  
47 of the samples. This is probably due to the segregation of the copolymerized side-chain functional  
48  
49 groups in HEMA copolymers,  $-NCH_3$  groups of DMAEMA and the  $-CF_3$  groups of TFEMA, are  
50  
51 segregated at the air/polymer interface. However, after 60 seconds, all the F-series samples were  
52  
53 more hydrophobic than PHEMA, whereas the N-series were more hydrophilic. The time  
54  
55  
56  
57  
58  
59  
60

dependence of WCA after placing a water droplet on polymer-coated substrates is shown in Figure S23. F9 presented the highest hydrophilicity in water among all samples in the F-series.

The functional group containing fluorine is segregated to the air/polymer interface because of its low cohesive force. However, upon contact with water, the fluorine-containing functional groups translocate into the more hydrophobic environment, the polymer matrix. Consequently, the surface is more easily reconstructed with a hydrophilic surface.<sup>51</sup> From the evaluation results by the captive bubble method as shown in Table 3, both F- and N-series were hydrophilized at the water/polymer interface. Therefore, the elemental analysis by XPS was conducted to determine the elemental composition at the interface.

**Table 3.** Contact angle<sup>a</sup> of all the HEMA copolymers used in the investigation.

Category	Code	Sessile drop (WCA)		Captive bubble (ACA)
		1s	60 s	24 h
Control	PHEMA	39.2 ±1.3	22.9 ±0.5	132.0 ± 6.5
N-series	N1	40.9 ±3.6	19.3± 1.0	146.6 ± 0.4
	N3	41.3 ±2.3	15.0 ±3.7	143.9 ± 0.8
	N5	44.7 ±6.4	15.1 ±3.4	150.0 ±1.5
	N7	43.0 ±2.6	10.1 ±0.3	146.6 ±1.5

	N10	49.3 ±4.6	14.4 ±4.5	149.2 ±0.4
	N25	48.3 ±5.0	13.5 ±2.8	146.9 ±1.9
F-series	F1	47.2 ±1.8	25.5 ±0.7	134.0 ±1.4
	F3	51.4 ±1.6	31.2 ±2.5	133.7 ±6.2
	F5	59.7 ±1.3	47.2 ±1.4	136.4 ±2.7
	F7	65.4 ±1.1	57.5 ±2.8	137.4 ±0.8
	F9	66.9 ±1.6	58.5 ±3.9	141.2 ±1.0
	F26	84.6 ±2.1	82.1 ±1.7	131.8 ±1.2
	F100	92.9 ±1.2	91.6 ±0.8	100.9 ±2.6

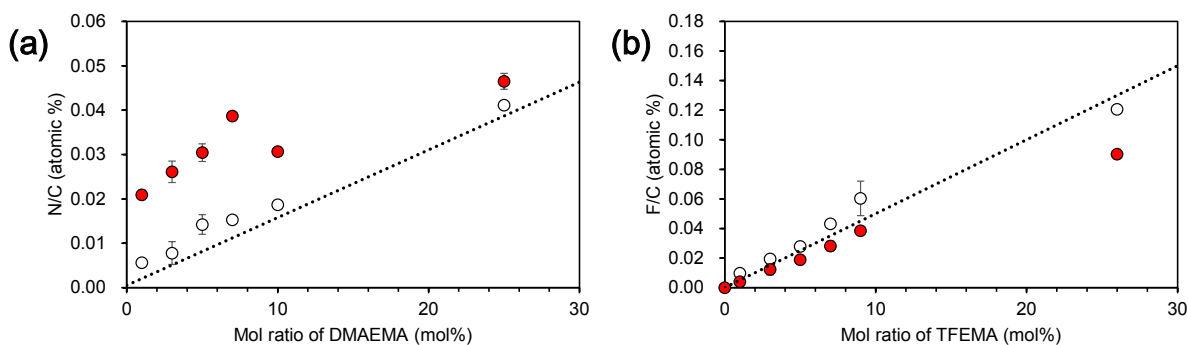
<sup>a</sup> WCA (sessile drop method) and ACA (captive bubble method). The data represent the means ± SD (n = 3).

## 6. XPS analyses of dry and hydrated HEMA copolymers.

The N25 coated substrate shows higher hydrophilicity in water (Table 3) and also the IWC of N25 is about twice higher than that of F9 (Table S1). However, N25 adsorbs twice as much amount of fibrinogen as compared to F9. This result for N25 was considered a singularity compared to other copolymers. In order to analyze the molecular orientation at the water/polymer interface, XPS measurement was performed using freeze-dried polymer-coated PET substrates from the water contact environment.

1  
2  
3 We have previously reported that PMEA copolymerized with a high  $T_g$  component  
4  
5  
6 maintains the hydrophilized surface even after freeze-drying and the vacuum process of  
7  
8  
9  
10 XPS measurement.<sup>30</sup> PHEMA has a high  $T_g$  in a dry state and the 8 wt% hydrated PHEMA  
11  
12  
13 shows  $T_g$  at about 50 °C. As the water content in hydrated PHEMA decreases during the  
14  
15  
16 freeze-drying process, the  $T_g$  is likely to be maintained above room temperature.  
17  
18  
19  
20  
21 Therefore, surface reconstruction was expected to be sufficiently slow to obtain the  
22  
23  
24 information reflecting the state of hydrated surface. Thus, the surface of novel HEMA  
25  
26  
27 copolymers that treated by the freeze-drying process was analyzed by XPS. The samples  
28  
29  
30  
31 were immersed in water for 1 hour before freeze-drying at room temperature and kept at  
32  
33  
34  
35 –30 °C for 16 hours under a vacuum condition of 20 Pa during freezing. To compare the  
36  
37  
38 distribution of the elements on the surfaces with and without priming, the samples without  
39  
40  
41  
42 freeze-drying were used as a control. The results are shown in Figure 6. In the case of HEMA  
43  
44  
45 copolymers with DMAEMA, the N/C ratio of copolymers were found to be higher than the  
46  
47  
48 theoretical ones in the hydrated state, probably due to the segregation of –NCH<sub>3</sub> group to the  
49  
50  
51 polymer/water interface. On the other hand, in the case of the copolymers containing TFEMA, the  
52  
53  
54 F/C ratio was lower than the theoretical value. Therefore, this can be interpreted that the functional  
55  
56  
57 groups containing fluorine atoms have translocated from the air/polymer interface into the polymer  
58  
59  
60

1  
2  
3 matrix. Based on the above results, the reason for a large amount of fibrinogen adsorbed on N25  
4 surface is because the positively charged  $-NCH_3$  group was segregated at the interface in the  
5 physiological environment. It is noteworthy that there are reports describing the mechanisms of  
6 fibrinogen adsorption onto the positively charged surface with electrostatic interaction. The core  
7 of fibrinogen is negatively charged and the core of fibrinogen attaches onto the surface by side-on  
8 adsorption.<sup>52</sup> In particular, the degree of adsorption and denaturation on N10 and N25 were  
9 increased. This is probably because the effect was prominently expressed by priming.



10  
11  
12  
13  
14  
15  
16  
17  
18  
19  
20  
21  
22  
23  
24  
25  
26  
27  
28  
29  
30  
31  
32  
33 **Figure 6.** Surface elemental analysis of N-series (a) or F-series (b) by XPS. The dotted  
34 line shows the theoretical value calculated from the composition ratio. The data represent  
35 the means  $\pm$  SD ( $n = 3$ ). White and red indicates before and after freeze drying, respectively.

### 46 47 **7. Novel molecular design of bio-inert hydrophilic polymers**

48  
49 Up until this section, the discussion has been focused on binary HEMA copolymers. Hydration  
50 state was changed with changes in mobility of hydrated polymer and water by copolymerizing a  
51 small amount of either amino or fluorine monomers. The change in the hydration state is

1  
2  
3 considered to be brought about by the changes in intra- and intermolecular interactions and was  
4 represented by the opposite effect in the case of N- and F-series. In order to verify whether this  
5 effect can coexist in a single copolymer, ternary copolymers (denoted as  $N_xF_y$ ) were synthesized  
6 and their physical properties were evaluated as shown in Table 1. Since  $N_xF_y$  exhibited an  
7 intermediate amount of EWC between  $N_x$  and  $F_y$ , the copolymers were likely affected by both  
8 TFEMA and DMAEMA (Table S1). Figure 7 shows the DSC heating profile of N5F5 under EWC  
9 condition as a typical example of a ternary copolymer, and the results for its binary analogs (N5  
10 and F5) are summarized in Table 4. Water molecules in N5 and F5 began to cold crystallize at  
11  $-31.1$  and  $-17.1$  °C, and their exothermic peaks appeared at  $-12.8$  and  $-8.1$  °C. On the other hand,  
12 cold crystallization of N5F5 started at a lower temperature than that of N5,  $-35.9$  °C, whereas its  
13 exothermic peak at  $-9.9$  °C was close to that of F5. Based on these results, we can conclude that  
14 the copolymers incorporating both amino and fluorine monomers simultaneously exhibit the  
15 effects observed independently for each binary HEMA copolymers. From the results of the surface  
16 elemental analysis (Figure S24), before and after freeze-drying, both N/C and F/C of  $N_xF_y$  showed  
17 the same behavior as that of the binary HEMA copolymers. Therefore, it can be considered that  
18 the copolymer containing both monomers reflects the properties of each copolymer in the hydrated  
19 state, not only in bulk but also in the water/polymer interface. Thus, the cold crystallization of  
20 water in the ternary copolymer appeared as the sum of water crystallization behavior in both binary  
21 copolymers, the crystallization of IW appeared in a wider temperature range as shown in Figure 7  
22 and Table 4. Therefore, the relationship between IWC and biological responses is examined in the  
23 following section. With the increase of IWC, improvement in the bio-inert properties is  
24 expected.<sup>14,27,29</sup>

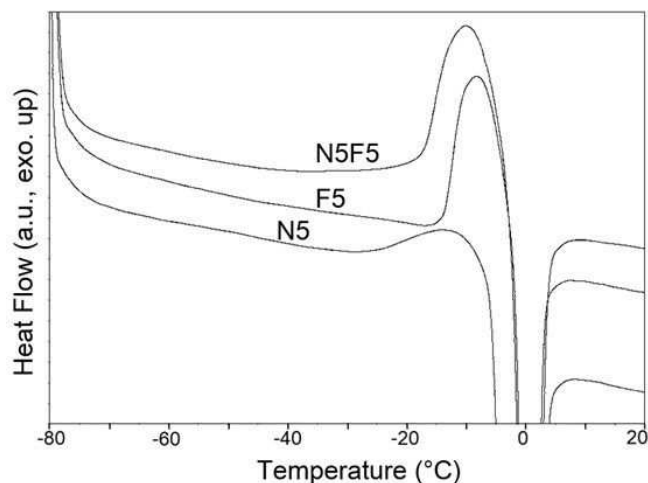


**Figure 7.** DSC heating profiles of N5, F5 and N5F5 at EWC conditions

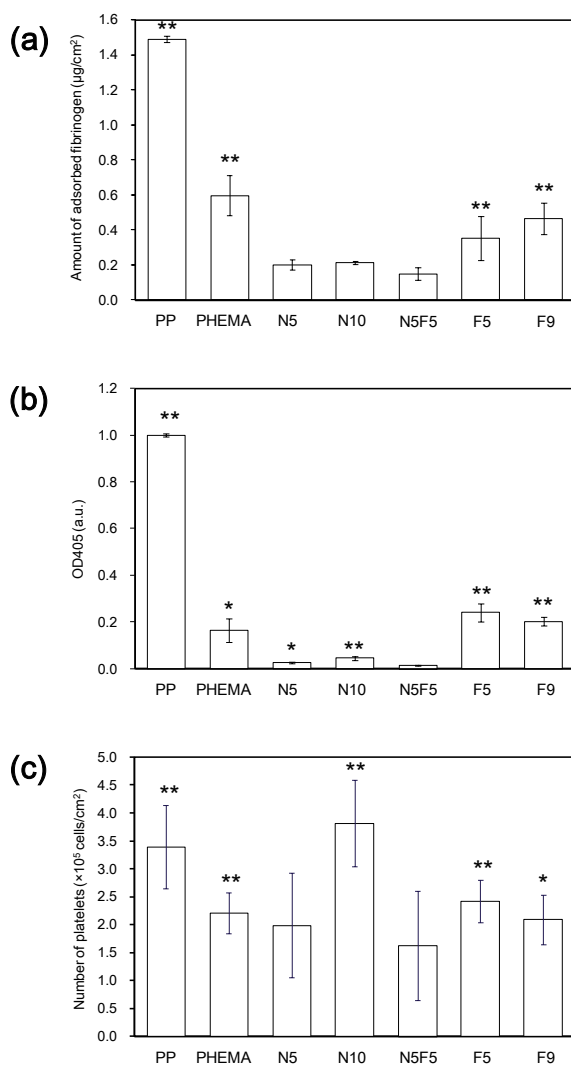
**Table 4.** Temperature range of cold crystallization and IWC in the heating process of N5, F5, and N5F5 at EWC condition.

	PHEMA	N5	N5F5	F5
Start of the cold crystallization (°C) <sup>a</sup>	-34.7	-31.1	-35.9	-17.1
Exothermic peak (°C)	-13.3	-13.7	-9.9	-8.1
IWC (wt%)	2.3	2.1	5.2	3.8

<sup>a</sup> The temperature of the beginning of the cold crystallization was identified from the inflection temperature.

Figure 8 shows the evaluated results for the amount of adsorbed fibrinogen, its denaturation degree, and the number of adhered human platelets. In almost all cases, the ternary copolymers containing the same amount of one or both foreign monomers were more bio-inert than the corresponding

1  
2  
3 binary copolymers. Similar effects were observed for N3F3 and are shown in Figure S25. These  
4  
5 results indicate the importance of introducing foreign monomers and the synergetic effect of IWC  
6  
7 increasing from different mechanisms of amino and fluorine groups in PHEMA. This IWC  
8  
9 increment may be the reason for the improvement of bio-inert properties of copolymers  
10  
11 synthesized herein.  
12  
13  
14



15  
16  
17  
18  
19  
20  
21  
22  
23  
24  
25  
26  
27  
28  
29  
30  
31  
32  
33  
34  
35  
36  
37  
38  
39  
40  
41  
42  
43  
44  
45  
46  
47  
48  
49  
50  
51 **Figure 8.** The amount of fibrinogen adsorption (a), the exposure degree of gamma chain of  
52  
53  
54 fibrinogen (b), and the number of human platelet adhesion (c) onto the surface of HEMA  
55  
56  
57  
58  
59  
60



1  
2  
3 copolymers and using surfaces with priming. PP is included as control surface. The data represent  
4  
5  
6  
7 the means  $\pm$  SD ( $n = 3$ ) of fibrinogen adsorption and denaturation and  $\pm$  SD ( $n = 11$ ) of the  
8  
9  
10 platelet adhesion. \*:  $P < 0.05$ , \*\*:  $P < 0.01$  vs. N5F5 substrate with priming.  
11  
12  
13  
14  
15  
16  
17

## 18 **Conclusions**

19  
20  
21 We have synthesized binary and ternary HEMA copolymers containing small amounts  
22  
23  
24 of DMAEMA and TFEMA by free radical polymerization. Although the homopolymers  
25  
26  
27 obtained from these two monomers did not show bio-inert properties, HEMA copolymers  
28  
29  
30 containing a small amount of these two monomers showed higher bio-inert properties than homo-  
31  
32  
33 PHEMA. By incorporating a small amount of amino or fluorine monomers into HEMA, the  
34  
35  
36 hydration state was changed.  
37  
38  
39

40 From the evaluation results of polymer and water mobility in the hydrated state, it is  
41  
42  
43 revealed that the incorporation of small amounts of foreign monomers loosens or fastens  
44  
45  
46 the water-polymer interaction in HEMA copolymers. This result can be interpreted as follows:  
47  
48  
49

50  
51 When hydrophilic DMAEMA was introduced to HEMA,  $NFW$  changed to  $IW$  and  $FW$ .  
52  
53  
54 Conversely, introduction of hydrophobic TFEMA to HEMA,  $FW$  changed to  $IW$  and  $NFW$ . Since  
55  
56  
57  
58  
59  
60

1  
2  
3 DMAEMA is positively charged in physiological environments, segregation of the charged  
4  
5  
6  
7 amino group to the water-polymer interface leads to more protein adsorption, denaturation,  
8  
9  
10 and platelet adhesion. For TFEMA, the fluorine with low cohesive energy was found to  
11  
12  
13 segregate rapidly to the air-polymer interface, effectively switch to the hydrophilized  
14  
15  
16 surface at the water-polymer interface upon hydration. Increased IWC and effective  
17  
18  
19 shielding of the *NFW* by *IW* contributes to improving the bio-inert properties of these  
20  
21  
22 copolymers. This interpretation of presented results is fully consistent with our previous  
23  
24  
25 investigations for MEA copolymers with small amount of fluorine monomers<sup>30</sup>. In addition,  
26  
27  
28 ternary copolymers containing TFEMA and DMAEMA exhibited an intermediate amount of EWC  
29  
30  
31 between N- and F-series. The ternary copolymer showed better bio-inert properties than that of  
32  
33  
34 binary copolymers having the same amount of foreign comonomers. This result can be  
35  
36  
37 interpreted as the higher IWC was achieved by the synergetic effect of DMAEMA and  
38  
39  
40 TFEMA in the ternary copolymers with HEMA. More investigations to confirm these  
41  
42  
43  
44  
45  
46 findings are already on going in our laboratory.  
47  
48  
49  
50  
51

## 52 **Associated Content**

53  
54  
55  
56  
57  
58  
59  
60

## Supporting Information

The Supporting Information is available free of charge on the ACS Publication website at

DOI:...

Detailed characterization data, DSC profiles, NMR spectra and SEC data for the discussed polymers.

## ORCID

Ryohei Koguchi: 0000-0003-0017-4783

Katja Jankova: 0000-0002-4218-064X

Shingo Kobayashi: 0000-0002-8357-8654

Daiki Murakami: 0000-0002-5552-4384

Masaru Tanaka: 0000-0002-1115-2080

## Acknowledgements:

1  
2  
3 This work was supported by JSPS KAKENHI Grant Number JP19H05720. Additionally, it  
4  
5  
6  
7 was partially supported by Dynamic Alliance for Open Innovation Bridging Human,  
8  
9  
10 Environment and Materials.

11  
12  
13  
14  
15 Project PROGRESS 100 from Kyushu University is acknowledged for financial support.

16  
17  
18 We thank BioSpin Division, Application Department, Bruker Japan K.K. for analysis with  
19  
20  
21  
22  $^1\text{H}$  pulse NMR and providing insight and expertise that greatly assisted the research.  
23  
24  
25  
26  
27  
28  
29

## 30 31 **Notes**

32  
33  
34  
35 The authors declare no competing financial interest.  
36  
37  
38  
39  
40  
41  
42

## 43 **ABBREVIATIONS**

### 44 45 **Materials**

46  
47 PEG Poly(ethylene glycol)  
48  
49 MPC 2-methacryloyloxyethyl phosphorylcholine  
50  
51 PMPC copolymer with 2-methacryloyloxyethyl phosphorylcholine and butyl methacrylate  
52  
53 PMEA Poly(2-methoxyethyl acrylate)  
54  
55 HEMA 2-hydroxyethyl methacrylate  
56  
57  
58  
59  
60

1		
2		
3	PHEMA	Poly(2-hydroxyethyl methacrylate)
4		
5	TFEMA	2,2,2-trifluoroethyl methacrylate
6		
7	DMAEMA	2-(dimethylamino)ethyl methacrylate
8		
9	PP	Polypropylene
10		
11	PET	polyethylene terephthalate
12		
13		
14		

### Analyses

15		
16		
17	NMR	Nuclear Magnetic Resonance
18		
19	GPC	Gel Permeation Chromatography
20		
21	DSC	Differential Scanning Calorimetry
22		
23	DDSC	temperature derivative of differential scanning calorimetry
24		
25	CA	Contact Angle
26		
27	WCA	Water in air Contact Angle
28		
29	ACA	Air in water Contact Angle
30		
31	XPS	X-ray Photoelectron Spectroscopy
32		
33	SEM	Scanning Electron Microscope
34		
35		
36		

### Interactions between water and polymers

37		
38		
39	<i>NFW(C)</i>	non-freezing water (content)
40		
41	<i>IW(C)</i>	intermediate water (content)
42		
43	<i>FW(C)</i>	free water (content)
44		
45	EWC	equilibrium water content
46		
47		
48		
49		
50		

---

51

52

53 <sup>1</sup> Ratner, B. D.; Bryant, S. J. Biomaterials: where we have been and where we are going. *Annu.*

54 *Rev. Biomed. Eng.* **2004**, *6*, 41–75.

55

56

57

58

59

60

1  
2  
3  
4  
5  
6 <sup>2</sup> Harris, J. M. E. *Poly(Ethylene Glycol) Chemistry, Biotechnical and Biomedical Applications*;  
7  
8 Springer US: New York, **1992**; p 385.

9  
10 <sup>3</sup> Holmlin, E.; Chen, X.; Chapman, R. G.; Takayama, S.; Whitesides, G. M. Zwitterionic SAMs  
11  
12 that resist nonspecific adsorption of protein from aqueous buffer. *Langmuir* **2001**, *17*, 2841–2850.

13  
14 <sup>4</sup> Han, D. K.; Park, K. D.; Ryu, G. H.; Kim, U. Y.; Min, B. G.; Kim, Y. H. Plasma protein  
15  
16 adsorption to sulfonated poly(ethylene oxide)-grafted polyurethane surface. *J. Biomed. Mater.*  
17  
18 *Res.* **1996**, *30* (1), 23–30.

19  
20 <sup>5</sup> Jeon, S. I.; Lee, L. H.; Andrade, J. D.; de Gennes, P. G. Protein—surface interactions in the  
21  
22 presence of polyethylene oxide: I. Simplified theory. *J. Colloid Interface Sci.* **1991**, *142*, 149-158.

23  
24 <sup>6</sup> McPherson, T.; Kidane, A.; Szleifer, I.; Park, K. Prevention of protein adsorption by tethered  
25  
26 poly(ethylene oxide) layers: Experiments and single-chain mean-field analysis. *Langmuir* **1998**,  
27  
28 *14*, 176-186.

29  
30 <sup>7</sup> Uchida, K.; Hoshino, Y.; Tamura, A.; Yoshimoto K.; Kojima S.; Yamashita K.; Yamanaka I.;  
31  
32 Otsuka H.; Kataoka K.; Nagasaki Y. Creation of a mixed poly (ethylene glycol) tethered-chain  
33  
34 surface for preventing the nonspecific adsorption of proteins and peptides. *Biointerphases* **2007**,  
35  
36 *2*, 126-130.

37  
38 <sup>8</sup> Ishihara K.; Ueda T.; Nakabayashi N. Preparation of phospholipid polymers and their properties  
39  
40 as polymer hydrogel membrane. *Polym. J.* **1990**, *22*, 355-360.

41  
42 <sup>9</sup> Kyomoto, M.; Moro, T.; Yamane, S.; Hashimoto, M.; Takatori, Y.; Ishihara, K. Poly (ether-ether-  
43  
44 ketone) orthopedic bearing surface modified by self-initiated surface grafting of poly (2-  
45  
46 methacryloyloxyethyl phosphorylcholine). *Biomaterials* **2013**, *34* (32), 7829–7839.

1  
2  
3  
4  
5  
6 <sup>10</sup> Ishihara, K. Bioinspired phospholipid polymer biomaterials for making high performance  
7 artificial organs. *Sci. Technol. Adv. Mater.* **2000**, *1* (3), 131–138.

8  
9  
10  
11 <sup>11</sup> Tanaka, M.; Motomura, T.; Kawada, M.; Anzai, T.; Kasori, Y.;Shiroya, T.; Shimura, K.; Onishi,  
12 M.; Mochizuki, A. Blood compatible aspects of poly(2-methoxyethylacrylate) (PMEA) –  
13 relationship between protein adsorption and platelet adhesion on PMEA surface. *Biomaterials*  
14 **2000**, *21* (14), 1471–1481.

15  
16  
17  
18  
19  
20 <sup>12</sup> Tanaka, M.; Motomura, T.; Kawada, M.; Anzai, T.; Kasori, Y.; Shimura, K.; Onishi, M.;  
21 Mochizuki, A.; Okahata, Y. A new blood-compatible surface prepared by poly(2-  
22 methoxyethylacrylate)(PMEA) coating-protein adsorption on PMEA surface. *Jpn J Artif Organs*  
23 **2000**, *29*, 209-216.

24  
25  
26  
27  
28  
29  
30 <sup>13</sup> Anzai, T.; Okumura, A.; Kawaura, M.; Yokoyama, K.; Oshiyama, H.; Kido, T.; Nojiri, C.  
31 Evaluation of the Biocompatibility of an In Vitro Test Using a poly(2-methoxyethyl acrylate)  
32 Coated Oxygenator. *Jpn J Artif Organs* **2000**, *9*, 73-77.

33  
34  
35  
36  
37  
38  
39  
40 <sup>14</sup> Sato, K.; Kobayashi, S.; Kusakari, M.; Watahiki, S.; Oikawa, M.; Hoshihara, T.; Tanaka, M. The  
41 Relationship Between Water Structure and Blood Compatibility in Poly(2-methoxyethyl Acrylate)  
42 (PMEA) Analogues. *Macromol. Biosci.* **2015**, *15* (9), 1296–1303.

43  
44  
45  
46  
47  
48  
49  
50 <sup>15</sup> Kobayashi, S.; Wakui, M.; Iwata, Y.; Tanaka, M. Poly( $\omega$ -methoxyalkyl acrylate)s:  
51 Nonthrombogenic Polymer Family with Tunable Protein Adsorption. *Biomacromolecules*, **2017**,  
52 *18* (12), 4214-4223.

1  
2  
3  
4  
5  
6 <sup>16</sup> Sato, K.; Kobayashi, S.; Sekishita, A.; Wakui, M.; Tanaka, M. Synthesis and Thrombogenicity  
7  
8 Evaluation of Poly(3-methoxypropionic acid vinyl ester): A Candidate for Blood-Compatible  
9  
10 Polymers. *Biomacromolecules* **2017**, *18* (5), 1609–1616.

11  
12  
13 <sup>17</sup> Tanaka, M.; Kobayashi, S.; Murakami, D.; Aratsu, F.; Kashiwazaki, A.; Hoshiba, T.;  
14  
15 Fukushima, K. Design of Polymeric Biomaterials: The “Intermediate Water Concept”. *Bull. Chem.*  
16  
17 *Soc. Jpn.* **2019**, *92* (12), 2043-2057.

18  
19  
20 <sup>18</sup> Ratner, B. D.; Hoffman, A. S.; Whiffen, J. D. Blood Compatibility of Radiation Grafted  
21  
22 Hydrogels. *Biomaterials, Med. Devices and Artif. Organs.* **1975**, *3* (1) 115-120.

23  
24  
25 <sup>19</sup> Martins, M.; Wang, D.; Ji, J.; Feng, L.; Barbosa, M. Albumin and Fibrinogen Adsorption on  
26  
27 PU–PHEMA Surfaces. *Biomaterials* **2003**, *24* (12), 2067–2076.

28  
29  
30 <sup>20</sup> Ratner, B. D.; Hoffman, A. S.; Hanson, S. R.; Harker, L. A.; Whiffen, J. D. Blood-compatibility-  
31  
32 water-content relationships for radiation-grafted hydrogels. *J. Polym. Sci., Polym. Symp.* **1979**, *66*  
33  
34 (1), 363–375.

35  
36  
37 <sup>21</sup> Okano, T.; Katayama, M.; Shinohara, I. The influence of hydrophilic and hydrophobic domains  
38  
39 on water wettability of 2-hydroxyethyl methacrylate - styrene copolymers. *J Appl Polym Sci.* **1978**,  
40  
41 *22* (2), 369-377.

42  
43  
44 <sup>22</sup> Senshu, K.; Kobayashi, M.; Ikawa, N.; Yamashita, S.; Hirao, A.; Nakahama, S. Time-Resolved  
45  
46 Surface Rearrangements of Poly(2-hydroxyethyl methacrylate-block-isoprene) in Response to  
47  
48 Environmental Changes *Langmuir* **1999**, *15* (5), 1754-1762.

49  
50  
51 <sup>23</sup> Senshu, K.; Kobayashi, M.; Ikawa, N.; Yamashita, S.; Hirao, A.; Nakahama, S. Relationship  
52  
53 between Morphology of Microphase-Separated Structure and Phase Restructuring at the Surface  
54  
55



of Poly[2-hydroxyethyl methacrylate-block-4-(7'-octenyl)styrene] Diblock Copolymers Corresponding to Environmental Change. *Langmuir* **1999**, *15* (5), 1763-1769.

<sup>24</sup> Kikuchi, A.; Karasawa, M.; Tsuruta, T.; Kataoka, K. Differential affinity of lymphocyte subpopulations toward PHEMA surface derivatized with a small amount of amino groups - Evaluation under the regulated shear stress *J. Colloid Interface Sci.* **1993**, *158*, 10-18.

<sup>25</sup> Tsuruta, T. On the role of water molecules in the interface between biological systems and polymers. *J. Biomater. Sci. Polym. Ed.* **2010**, *21*, 1831-1848.

<sup>26</sup> [www.soft-material.jp/en/](http://www.soft-material.jp/en/)

<sup>27</sup> Tanaka, M.; Mochizuki, A.; Ishii, N.; Motomura, T.; Hatakeyama, T. Study of Blood Compatibility with Poly(2-methoxyethyl acrylate). Relationship between Water Structure and Platelet Compatibility in Poly(2-methoxyethyl acrylate-co-2-hydroxyethyl methacrylate). *Biomacromolecules* **2002**, *3* (1), 36-41.

<sup>28</sup> Hirota, E.; Ute, K.; Uehara, M.; Kitayama, T.; Tanaka, M.; Mochizuki, A. Study on blood compatibility with poly(2 - methoxyethylacrylate)-relationship between surface structure, water structure, and platelet compatibility in 2 - methoxyethylacrylate/2 - hydroxyethylmethacrylate diblock copolymer. *J. Biomed. Mater. Res.* **2006**, *76A*, 540-550.

<sup>29</sup> Javakhishvili, I.; Tanaka, M.; Ogura, K.; Jankova, K.; Hvilsted, S. Synthesis of graft copolymers based on poly(2-methoxyethyl acrylate) and investigation of the associated water structure. *Macromol Rapid Commun.* **2012**, *33* (4), 319-325.

<sup>30</sup> Koguchi, R.; Jankova, K.; Tanabe, N.; Amino, Y.; Hayasaka, Y.; Kobayashi, D.; Miyajima, T.; Yamamoto, K.; Tanaka, M. Controlling the hydration structure with small amount of fluorine to

1  
2  
3  
4  
5  
6 produce blood compatible fluorinated poly(2-methoxyethyl acrylate). *Biomacromolecules*, **2019**,  
7  
8 *20*, 2265-2275.

9  
10 <sup>31</sup> Zhao, Z.; Ni, H.; Han, Z.; Jiang, T.; Xu, Y.; Lu, X.; Ye, P. Effect of Surface Compositional  
11  
12 Heterogeneities and Microphase Segregation of Fluorinated Amphiphilic Copolymers on  
13  
14 Antifouling Performance. *ACS Appl. Mater. Interfaces* **2013**, *5*, 7808–7818.

15  
16  
17 <sup>32</sup> Ostuni, E.; Chapman, R. G.; Holmlin, E.; Takayama, S.; Whitesides, G. M. A survey of  
18  
19 structure– property relationships of surfaces that resist the adsorption of protein. *Langmuir* **2001**,  
20  
21 *17*, 5605–5602.

22  
23  
24 <sup>33</sup> Chapman, R. G.; Ostuni, E.; Takayama, S.; Holmlin, R. E.; Yan, L.; Whitesides, G. M.  
25  
26 Surveying for Surfaces that Resist the Adsorption of Proteins. *J. Am. Chem. Soc.* **2000**, *122*,  
27  
28 8303–8304.

29  
30  
31 <sup>34</sup> Cotanda, P.; Wright, D. B.; Tyler, M.; O'Reilly, R. K. A Comparative Study of the Stimuli-  
32  
33 Responsive Properties of DMAEA and DMAEMA Containing Polymers. *J. Polym. Sci., Part A:*  
34  
35 *Polym. Chem.* **2013**, *51*, 3333–3338.

36  
37  
38 <sup>35</sup> Samsonova, O.; Pfeiffer, C.; Hellmund, M.; Merkel, O. M.; Kissel, T. Low Molecular Weight  
39  
40 pDMAEMA-block-pHEMA Block-Copolymers Synthesized via RAFT-Polymerization: Potential  
41  
42 Non-Viral Gene Delivery Agents? *Polymers* **2011**, *3* (2), 693–718.

43  
44  
45 <sup>36</sup> Xu, F. J.; Li, H. Z.; Li, J.; Zhang, Z. X.; Kang, E. T.; Neoh, K. G. Star-Shaped Cationic Polymers  
46  
47 by Atom Transfer Radical Polymerization from  $\beta$ -Cyclodextrin Cores for Nonviral Gene Delivery.  
48  
49 *Biomaterials* **2008**, *29*, 3023–3033.

50  
51  
52 <sup>37</sup> Calucci, L.; Forte, C.; Ranucci, E. Water/Polymer Interactions in a Poly(amidoamine) Hydrogel  
53  
54 Studied by NMR Spectroscopy. *Biomacromolecules* **2007**, *8*, 2936–2942.

- 
- 1  
2  
3  
4  
5  
6 38 Morita, S.; Kitagawa, K.; and Ozaki, Y. Hydrogen-bond structures in poly(2-hydroxyethyl  
7 methacrylate): Infrared spectroscopy and quantum chemical calculations with model compounds.  
8 *Vib.Spectrosc.* **2009**, *51*, 28-33.  
9  
10  
11  
12 39 Nakamura, K., Hatakeyama, T., and Hatakeyama, H. Effect of Water on the Glass Transition of  
13 Styrene-Hydroxystyrene Copolymers. *Kobunshi Ronbunshu*, **1981**, *38* (11), 763-767.  
14  
15  
16 40 Nakamura, K.; Hatakeyama, T.; and Hatakeyama, H. Differential scanning calorimetric studies  
17 on the glass transition temperature of polyhydroxystyrene derivatives containing sorbed water.  
18 *Polymer*, **1981**, *22*, 473-476.  
19  
20  
21  
22 41 Meakin, J. R.; Hukins, D. W. L.; Imrie, C. T.; Aspden, R. M. Thermal analysis of poly(2-  
23 hydroxyethyl methacrylate) (pHEMA) hydrogels. *J. Mater. Sci. Mater. Med.* **2003**, *14*, 9–15.  
24  
25  
26 42 Sugisaki, M.; Sugg, H.; Seki, S. Calorimetric Study of the Glassy State. III. Novel Type  
27 Calorimeter for Study of Glassy State and Heat Capacity of Glassy Methanol. *Bull. Chem. Soc.*  
28 *Jpn.* **1968**, *41*, 2586.  
29  
30  
31  
32 43 Kim, Y. S.; Dong, L.; Hickner, M. A.; Glass, T. E.; Webb, V.; McGrath, J. E. State of Water in  
33 Disulfonated Poly(arylene ether sulfone) Copolymers and a Perfluorosulfonic Acid Copolymer  
34 (Nafion) and its Effect on Physical and Electrochemical Properties. *Macromolecules* **2003**, *36*,  
35 6281–6285.  
36  
37  
38 44 Kelley, F. N.; Bueche, F. J. Viscosity and glass temperature relations for polymer - diluent  
39 systems. *Polym. Sci.* **1961**, *L*, 549-556.  
40  
41  
42 45 Tran, T., Lin, C., Chaurasia, S., and Lin, H. Elucidating the relationship between states of water  
43 and ion transport properties in hydrated polymers. *Journal of Membrane Science*, **2019**, *574*, 299–  
44 308.  
45  
46  
47  
48  
49  
50  
51  
52  
53  
54  
55  
56  
57  
58  
59  
60

1  
2  
3  
4  
5  
6 46 Hill, D. J. T.; Whittaker, A. K.  $^1\text{H}$  NMR Study of the States of Water in Equilibrium  
7  
8  
9 Poly(HEMA-co-THFMA) Hydrogels. *Biomacromolecules* **2002**, *3*(5), 991-997.

10  
11  
12  
13 47 Bloembergen, N.; Purcell, E. M.; Pound, R. V. Relaxation Effects in Nuclear Magnetic  
14  
15  
16 Resonance Absorption. *Phys. Rev.* **1948**, *73*, 679.

17  
18  
19  
20 48 Yamada-Nosaka, A.; Ishikiriyama, K.; Todoki, M.; Tanzawa, H.  $^1\text{H}$ -NMR studies on  
21  
22  
23 water in methacrylate hydrogels. I. *J. Appl. Polym. Sci.* **1990**, *39*, 2443–2452.

24  
25  
26 49 Rohrer, M.; Bauer, H.; Mintorovitch, J.; Requardt, M.; Weinmann, H.-J. Comparison of  
27  
28  
29 Magnetic Properties of MRI Contrast Media Solutions at Different Magnetic Field Strengths.  
30  
31 *Invest. Radiol.* **2005**, *40*, 715–724.

32  
33  
34 50 Tanaka, M.; Mochizuki, A. Effect of water structure on blood compatibility - Thermal analysis  
35  
36 of water in poly(meth)acrylate. *J. Biomed. Mater. Res.* **2004**, *68A* (4), 684–695.

37  
38  
39 51 Takahashi, S.; Kasemura, T.; Asano, K. Surface molecular mobility for copolymers having  
40  
41 perfluorooctyl and/or polyether side chains via dynamic contact angle. *Polymer* **1997**, *38* (9) 2107-  
42  
43 2111.

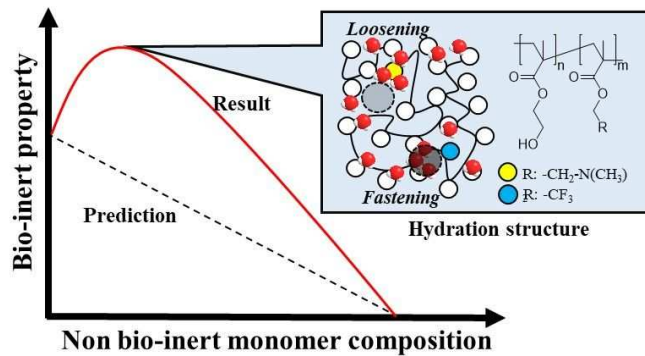
44  
45  
46 52 Żeliszewska, P.; Bratek-Skicki, A.; Adamczyk, Z.; Cieśla, M. Human Fibrinogen  
47  
48  
49 Adsorption on Positively Charged Latex Particles. *Langmuir* **2014**, *30*(37), 11165–11174.  
50  
51  
52  
53  
54  
55  
56  
57  
58  
59  
60

1  
2  
3  
4  
5  
6  
7  
8  
9  
10  
11  
12  
13  
14  
15  
16  
17  
18  
19  
20  
21  
22  
23  
24  
25  
26  
27  
28  
29  
30  
31  
32  
33  
34  
35  
36  
37  
38  
39  
40  
41  
42  
43  
44  
45  
46  
47  
48  
49  
50  
51  
52  
53  
54  
55  
56  
57  
58  
59  
60

---

For Table of Comments Use Only

1  
2  
3  
4  
5  
6 Table of Contents Graphic.  
7  
8  
9



26 Understanding the effect of hydration on the bio-inert properties of HEMA copolymers with  
27 small amounts of amino- or/and fluorine-containing monomers  
28  
29

30  
31  
32  
33  
34  
35 *Ryohei Koguchi, Katja Jankova, Yuki Hayasaka, Daisuke Kobayashi, Yosuke Amino, Tatsuya*  
36 *Miyajima, Shingo Kobayashi, Daiki Murakami, Kyoko Yamamoto, Masaru Tanaka\*\**  
37  
38  
39  
40  
41  
42  
43  
44  
45  
46  
47  
48  
49  
50  
51  
52  
53  
54  
55  
56  
57  
58  
59  
60